Removing Speckles Selectively from Iris Images to Improve Pupil Location Using 2D Gabor Filters

Chunxian Song, Guangzhu Xu*, Chunlin Li and Jing Jing

College of Computer and Information Technology, China Three Gorges University, Yichang, Hubei of P.R. China
songchunxian0419@163.com;xugzhu@gmail.com;lichunlin0921@126.com; jingjinzhengxi@163.com

Abstract

Removing speckles is a key step for accurate pupil location in an iris recognition system. This paper proposed an algorithm to detect speckles in pupil area based on 2D Gabor filters first. Then the speckles were replaced selectively with the average intensity of a fixed square region. Finally, a novel evaluation index was introduced, which improved the pupil location accuracy rate of our former pupil location algorithm. In the widely used CASIA v3.0 iris database, the pupil location accuracy rate was improved from 97.44% to 99.55%. And in several other commonly used iris test databases with less or without speckles, this method maintained the former location accuracy. The experimental results show that our algorithm has satisfactory performance, robustness and versatility.

Keywords: *2D Gabor filters, speckles removing, pupil location, iris recognition*

1. Introduction

Iris is an annular portion between the pupil and the white sclera (Figure 1. (a)), and contains rich textural information [1]. The identity recognition based on iris is widely regarded as one of the most promising biometric technologies in the 21st century [2-5].

In an iris recognition system, to segment iris area (termed as iris location) is a critical step which includes inner location (pupil location) and outer location (iris outer boundary location). The accuracy rate of pupil location directly affects outer boundary location, and further affects the validity of iris segmentation and the performance of the whole iris recognition system. However, due to the impact of image capturing environment, there are often speckles in pupil area (Figure 1 (b)). A large number of speckles would affect the accuracy rate of pupil location (Figure 1 (c, d)) dramatically.

In view of the importance of pupil location, many experts have done a lot of researches on it. Daugman [2] used the integral-differential operator to locate the pupil. By changing integral paths, the search operator could detect the circle with the biggest change of average intensity. To search for the feeble pupil edge, Daugman [2] adopted a Gaussian smooth function with small standard deviation. Wildes [3] used the canny operator to obtain the edge information of an image, then used the circle Hough transformation to extract points to fit the pupil edge, and achieved pupil location. But neither of the two classical location algorithms is suitable to the case of pupil with speckles, as shown in Figure 1 (c-d).

* Corresponding author: Guangzhu Xu
Telephone number: 86-15971636485

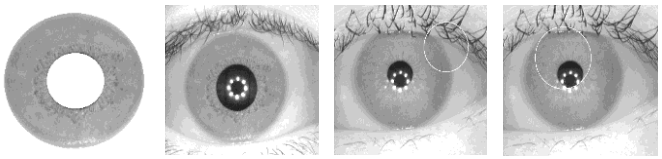

(a) (b) (c) (d)

Figure 1. (a) The iris between the pupil and the white sclera; (b) An image with a lot of speckles in pupil area; (c) The pupil location result by Daugman's method [2]; (d) The pupil location result by Wildes' method [3]

A large number of speckles would affect the accuracy rate of pupil location, so they should be moved out [6-10]. Tieniu Tan et al. [6] chose an appropriate threshold to obtain the binary image, and then used bilinear interpolation to fill the specula reflection. However, this method only fills reflection roughly, so the bright eyelid areas may be also detected. Walid Aydi etc. [7] used a mathematical morphology operator to process the images in CASIA v3.0 iris database. After binarization and dilating, linear interpolation was utilized to fill the speckles. But they do not consider its validity to the pupil location.

Our former iris location algorithm was fast and robust [4, 5], but CASIA v3.0 iris database was not been published at that time, so it did not take full account of the pupil with a large number of speckles. Now, the CASIA v3.0 database is available, in order to improve the adaptability of our location algorithm, the former method should be improved.

This paper selected the real parts of four 2D Gabor filters with equal size and different directions to filter an image respectively, and then superimposed the four filtered images to find all possible speckles. And then they were replaced with their surrounding average intensities in the original image. Finally, the Gaussian smooth function was utilized for the filled image, which is a necessary step for gradient-based location algorithm [2], and the pupil location was carried out on the smoothed image.

This paper consisted of three parts: at first the 2D Gabor filter was described, whose real part is especially suitable for finding the speckles in pupil area. After finding candidate speckles, they were selectively replaced by the average intensities of the square areas centered with the corresponding speckle. In the final part, we introduced an evaluation index to improve former location algorithm further. The experimental results showed that the speckle removing algorithm was very effective, and it improved the accuracy rate of pupil location from 97.44% to 99.55% in CASIA v3.0 iris database.

2. 2D Gabor Filter

The mathematical model of 2D Gabor was first proposed by Daugman in [11]. He found that 2D Gabor wavelet has good time-frequency resolution characteristic, which is suitable for image processing and pattern recognition [12]. The equations of the 2D Gabor filter in the space domain are as follows：

$$G(x,y) = g(x,y) \cdot s(x,y) \tag{1}$$

$$g(x,y) = e^{-\pi[(x-x_0)^2/a^2+(y-y_0)^2/b^2]} \tag{2}$$

$$s(x,y) = e^{-2\pi i[u_0(x-x_0)+v_0(y-y_0)]} \tag{3}$$

where g (x, y) is a two-dimensional Gaussian function, s (x, y) is a complex sinusoidal function. (x_0, y_0) represents the position of Gaussian window center, a and b control the width and length of the Gaussian window. (u_0, v_0) defines the frequency (($u_0^2+v_0^2)^{1/2}$) and direction (arctan (v_0/u_0)) of the modulation. The real and imaginary parts of G(x, y) are shown in Figure 2 (a) and (b). It can be found from Figure 2 (c) that the middle area is greater than 0 and the peripheral area is less than 0, which is similar to the speckles in pupil area. By selecting proper parameters, we could make the middle area have similar size with speckles. The middle area corresponded to speckles, while the peripheral area corresponded to non-speckles. We then chose the real part to filter the image, and the pixels with greater value were considered as the probable speckles in pupil area.

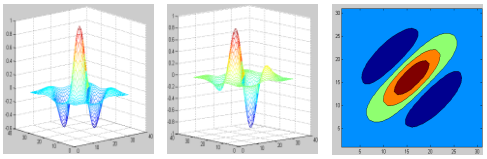

(a) (b) (c)

Figure 2. (a-b) The real and imaginary parts of 2D Gabor filter, in which $x_0=y_0=0$, a=b=15, f=1/15, θ=3π/4; (c) Contour map of the real part

3. Finding and Removing the Speckles in Pupil Area using 2D Gabor Filters

In order to find the speckles in pupil area, in our study, we filtered an eye image using the real part of a 2D Gabor filter first. The pixels in speckles had higher intensity value than others, this was similar to the real part of the 2D Gabor filter. So after filtering, the pixels in speckles would appear brighter than others. The eyelid areas and their surrounding pixels were all in great intensity. So their filtering results were small, and the pixels in eyelid areas would not be considered as speckles. To emphasize the possible speckle areas further and eliminate the effect from eyelashes, we selected the real parts of four 2D Gabor filters with different directions. Subsequently, the filtered results of the four different directions were superimposed and normalized to prepare for the following binarization.

Then, after careful experiments, an appropriate threshold was chosen to get the binary image and possible speckles. Because the filtered image was normalized, the threshold could be fixed. But some possible speckles might not be detected because of the great intensity variance in speckle areas. So we dilated the binary image to expand the speckles using octagonal morphological operator so that all speckles could be detected. Dilating operation could take some non-speckle area as speckles, but they would be removed in our following selective filling stage. The process of detecting the speckles is illustrated in Figure 3.

To remove the speckles (replaced or filled them with other intensity), we needed to determine which pixels were speckles. The pixels which were near to the pupil boundary should not be filled. Otherwise, it would affect the accuracy rate of pupil location. For every possible speckle, we calculated the average intensity in a square centered with it (counting only pixels of the original image which correspond to the black ones in the dilated image). If the average intensity in the square was less than 0.5, we could determine that the pixel was in pupil area, and then filled it with the average intensity. Otherwise, it might be near to the pupil edge. Then we should not fill it. The result after selective filling is shown in Figure 4. The filled speckles were not very smooth at the area edge. So the image was processed with a

Gaussian smoothing filter. After that the intensity of the filled pixel was replaced with the corresponding one in the

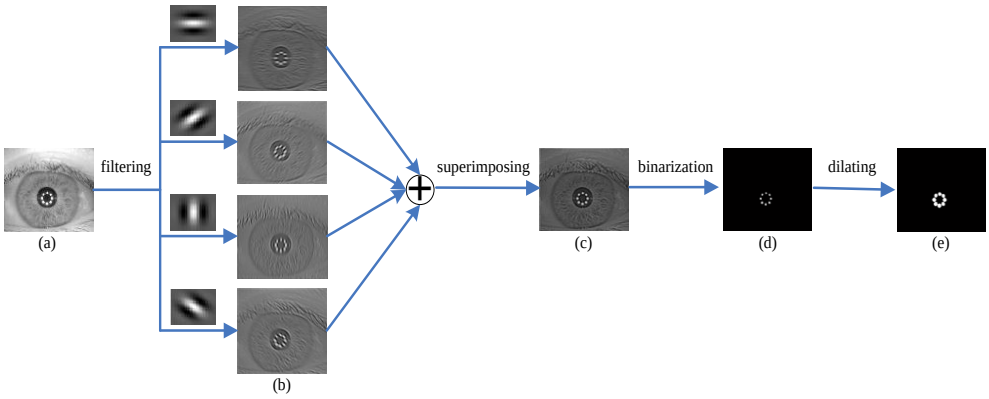

Figure 3. Detecting the speckles (a) The original image; (b) Four filtered results with the real parts of 2D Gabor filters in the directions of 0、π/4、π/2、3π/4; (c) Superimposed result of the four filtered images; (d) Binary result of the superimposed image; (e) Dilated result of the binary image

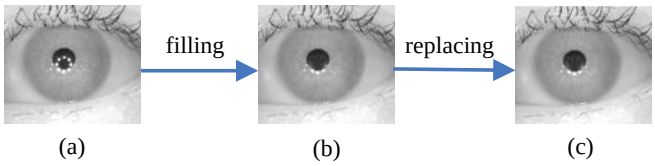

Figure 4. Removing the speckles (a) The original image; (b) The result after filling selectively the speckles in pupil area; (c) The result after replacing the filled pixels with corresponding ones in the smoothed image

smoothed image. And then we could get the final eye image with speckles in pupil area being removed selectively.

4. Pupil Location After Removing Speckles

The pupil boundary can be regarded as a circle. Pupil location is to determine the center and radius of the circle [4, 5]. It is a key step for iris recognition. The location accuracy rate would affect directly the performance of an iris recognition system. An excellent pupil location algorithm should be fast, accurate and universal. It should also tolerate speckles and eyelash occlusion.

After filling the speckles in the pupil area, we referred to our former location method [4, 5] (as shown in Figure 5). First, we divided the filled image into a number of small squares with a fixed size. And the one with the minimum average intensity was detected. Then, we used the minimum average intensity with a correction value as the threshold to get binary filled image (removing the speckles in pupil area). To eliminate possible eyelashes near the pupil and some possible speckles in the pupil, we adopted the processing of erosion and seed filling of mathematical morphology [4, 5]. At last, we expanded subtly the detected square in the binary image to get four pupil boundaries (i.e. top, bottom, left and right). And then the center and the radius of the pupil could be calculated according the four boundaries.

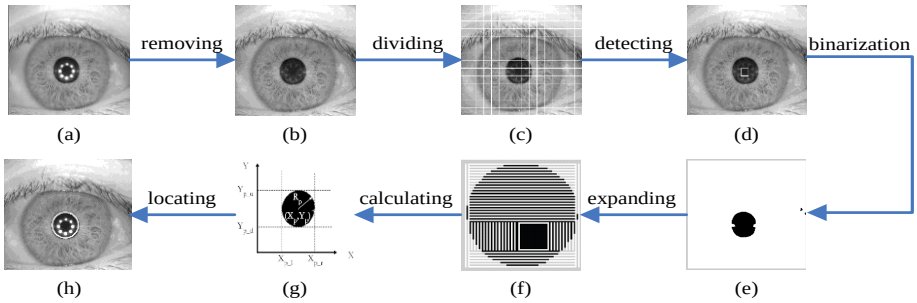

Figure 5. The pupil location (a) The eye image; (b) The image after removing speckles; (c) The divided image; (d) The square with the minimum average intensity; (e) The binary filled image; (f) The process of expanding the binary image with the referred square; (g) Calculating the center and the radius of the pupil; (h) The pupil location result

In order to improve our former location algorithm [4, 5] further, we introduced an evaluation index. To reduce the impact of intensity variation in the pupil area, we added respectively four correct values on the threshold in binary processing. Therefore four location results were gotten from the same image. Next step was to select the relatively accurate one. In each case, we calculated the average intensity (i.e. $inner_k$) within a circular area whose center and radius were the pupil center and the pupil radius in the binary image (the circular area in Figure 6). And then we calculated the average intensity (i.e. $outer_k$) within a square whose center and side length were the pupil center and the pupil diameter (the shaded area in Figure 6). Their mathematical expressions were given in (5) and (6).

$$D_k = outer_k - inner_k \tag{4}$$

$$inner_k = \frac{\sum I_i(x,y)}{\pi r^2} \tag{5}$$

$$outer_k = \frac{\sum I_o(x,y)}{4r^2 - \pi r^2} \tag{6}$$

where k=1, 2, 3, 4. I_i (x, y) was the intensity of the pixel in the circle area in the binary image and I_o (x, y) was the intensity of the pixel in the shaded area. When D_k in (6) was the maximum one under the k^{th} location result, the corresponding center and radius were considered as the final location results. The process is shown in Figure 7.

In our former method [4, 5], choosing the divided block size is crucial. If there are many speckles in pupil area, the smaller block would fall into the surrounding of the speckles in pupil area when it is used to find the four pupil boundaries by extending its edges towards four directions. In this situation, we should choose a larger one in case the block having the minimum average intensity fell into the surrounding of the speckles in the pupil area. However, if we use a too large block size, the block with the minimum average intensity may be not in pupil. And we could not use it to detect the pupil. In order to improve the versatility of our pupil location algorithm, four different sizes were selected to divide the filled images. We then located respectively the pupil in the same image, apply the evaluation index again. And the most accurate pupil location result could be gotten from 16 location ones, as shown in Figure 8.

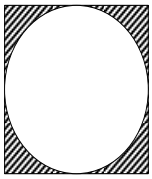

Figure 6. The average intensity $inner_k$ in the circle and the average intensity $outer_k$ in the shaded area

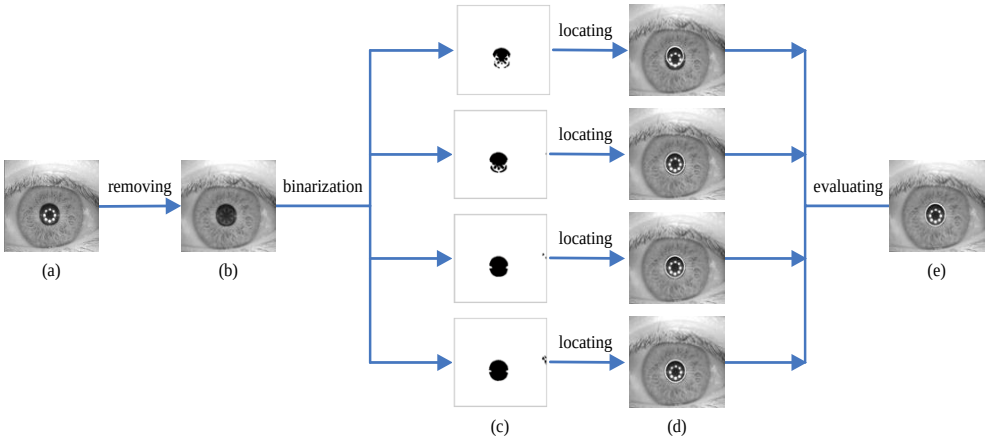

Figure 7. The process of applying the evaluation index under a fixed size (a) The original image; (b) The image after removing speckles in pupil area; (c) The binary filled images, the threshold values are the smallest average intensity plus four correction values (12, 20, 28 and 36); (d) Four pupil location results based on the corresponding binary images; (e) The pupil location result after applying the evaluation index

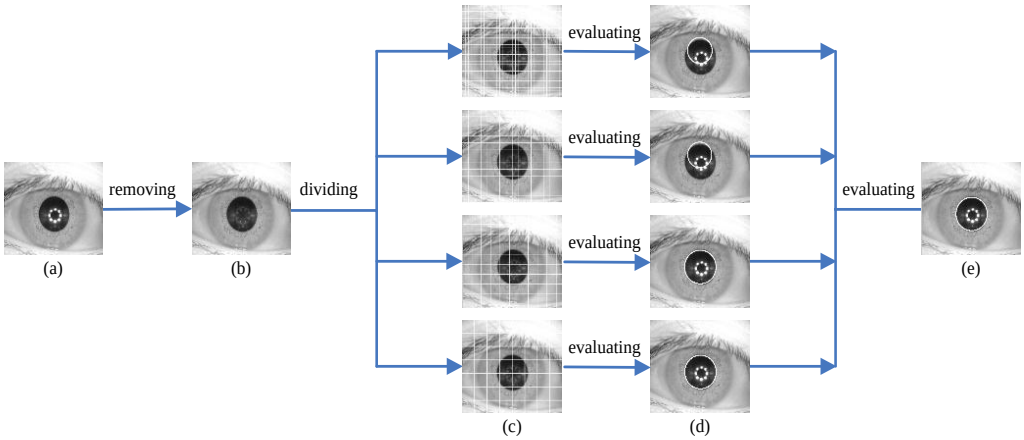

Figure 8. The process of applying the evaluation index under four sizes (a) The original image; (b) The image after removing speckles in pupil area; (c) The divided filled image with 10, 20, 30 and 40; (d) The location result after applying the evaluation index; (e) The final pupil location result after applying the evaluation index again

5. Experimental Results and Discussion

In our experiments, we selected the widely used CASIA v3.0 iris database [13], which consists of three subsets, and has a total of 22051 iris images coming from more than 700 subjects. The images of subset1 have rich textural information. Subset1 includes CASIA v1.0, but with a large number of speckles in pupil area (as shown in Figure 1 (b)). The subset2 introduces more intra-class variations by turning on/off a lamp nearby subject, and is used to study non-linear deformation model of iris pattern. Subset3 includes images from 100 pairs of twins, and it is mainly used to study the relationship between the iris and the gene. We chose the widely used subset1 [7, 9] to evaluate the proposed speckles removing method.

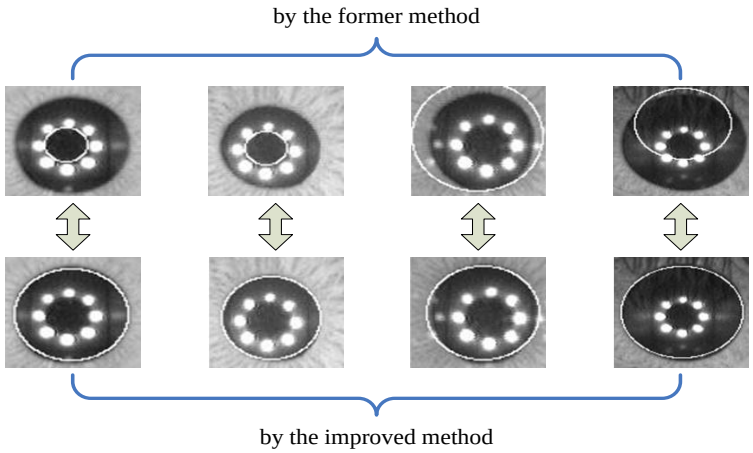

Figure 9. The Pupil Location Results Before and After Removing the Speckles

To illustrate the effectiveness of the proposed speckles removing method which improved the accuracy rate of pupil location, we had done a lot of comparing experiments on the pupil location results before and after removing speckles, as shown in Figure 9 (for clarity, the images are cut appropriately). It could be seen that, due to the speckles in pupil area, false pupil boundaries sometimes were found in the expanding process of our location method [4, 5]. It caused directly the failure of pupil location. Because considering the speckles in pupil area and filling selectively them in our new proposed algorithm, the disturbance of speckles was effectively reduced. So we achieved the purpose of accurate pupil location.

With the proposed algorithm, the accuracy rate of pupil location could reach 99.55% in CASIA v3.0 iris database. It could be seen from Figure 10 that the algorithm had a good performance for images with various speckles in pupil area (Figure 10 (a) - (c)). But when the upper or lower eyelid covered the iris too severely, the pupil itself lacked of boundary information. In this case, our algorithm was not able to locate the pupil accurately (Figure 10 (d)). When too many speckles were near the pupil boundary, our method possibly did not determine whether it was within or outside the pupil (Figure 10 (e)). In addition we regarded the pupil boundary as an ideal circle, but not all the boundaries were similar to circles, in these cases the proposed method could not find a circle to fit completely the pupil edge (Figure 10 (f)). But the extent of non-fitting was small for available eye images.

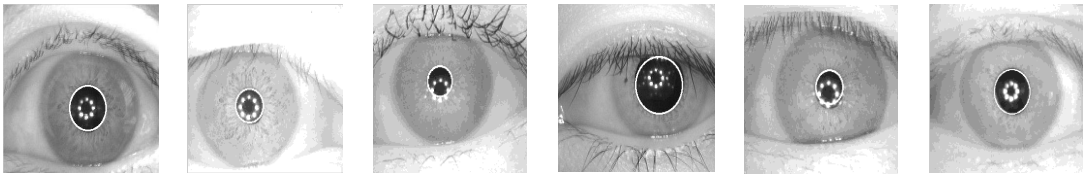

Figure 10. The pupil location results in CASIA v3.0 (a-c) Excellent pupil location results by our improved method; (d) Failure because of serious occlusion by the upper eyelid; (e) Failure because of too complex speckles; (f) Failure because of the irregular pupil shape

Table 1. The Pupil Location Accuracy Rates Before and After Removing Speckles in Several Iris Databases

	CASIA v3.0 [13]	CASIA v1.0 [16]	Bath [14]	MMU v1.0 [15]
Database capacity	2655	756	1000	450
Speckles in the pupil	with a lot of speckles	without speckles	with less speckles	with less speckles
Location accuracy using the former method [4]	97.44%	99.60%	100%	99.56%
Location accuracy using the improved method	99.55%	99.60%	100%	99.56%

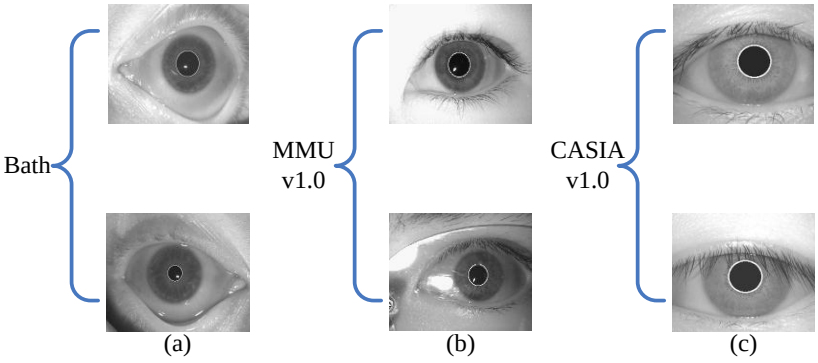

Figure 11. (a-b) The pupil location results in Bath; (c-d) The pupil location results in MMU v1.0; (e-f) The pupil location results in CASIA v1.0

The pupil location accuracy rates in different iris databases were shown in Table 1. In the table, with the help of the proposed method of removing speckles, the accuracy rate of pupil location in CASIA v3.0 was improved effectively. In the Bath [14] and MMU v1.0 [15] iris databases, there are only some small speckles in pupil area, and the images in CASIA v1.0 [16] have no speckle with manual processing [17]. The former pupil location algorithm has certain ability of anti-speckles. So the improved algorithm

could not improve significantly the accuracy rate of pupil location. Some sample images of pupil location in different iris databases were shown in Figure 11.

6. Conclusions

This paper proposed an algorithm of removing speckles by combining 2D Gabor filters and morphological techniques. Because only the speckles in pupil area are removed, the inaccurate pupil locations caused by speckles in it are reduced greatly. In order to enhance the robustness of our location algorithm, a pupil location evaluation index was introduced. The experimental results in CASIA v3.0, Bath, MMU v1.0 and CASIA v1.0 iris test databases show that the proposed algorithm can improve effectively the accuracy rate and robustness of the pupil location.

Acknowledgements

Authors wish to acknowledge institute of Automation, Chinese Academy of Sciences for providing CASIA v1.0 and v3.0 iris databases. Authors would also like to thank institute of Intelligent Vision and Image Information of China Three Gorges University for providing experimental devices. This paper is supported by the project (Q20111204) from Hubei Provincial department of education.

References

[1] Al. Muron and J. Pospisil, "The human iris structure and its usages", Acta Univ., Palacki, Phisica. 39 **(2000)**.

[2] J. Daugman, "High confidence visual recognition of persons by a test of statistical independence", IEEE Transactions on Pattern Analysis and Machine Intelligence, 11, 15, **(1993)**.

[3] R. Wildes, "Iris recognition: An emerging biometric technology", Proceedings of the IEEE, **(1997)** September, pp. 1348–1363; Princeton, America.

[4] G. Xu, Z. Zhang and Y. Ma, "Automatic iris segmentation based on local areas", The 18th International Conference on Pattern Recognition, **(2006)**, pp. 505-508, HongKong, China.

[5] G. Xu, Z. Zhang and Y. Ma, "A Novel and Efficient Method for Iris Automatic Location", Journal of China University of Mining & Technology, 17, 3, **(2007)**.

[6] Z. He and T. Tan, "Toward accurate and fast iris segmentation for iris biometrics", IEEE Transactions on Pattren Analysis and Machine Intelligence, 31, 9, **(2009)**.

[7] W. Aydi, N. Masmoudi and L. Kamoun, "New corneal reflection removal method used In Iris Recognition System", World Academy of Science, Engineering and Technology, 77, **(2011)**.

[8] S. J. Pundlik, "Non-ideal iris segmentation using graph cuts", IEEE Computer Society Conference on Computer Vision and Pattern Recognition Workshops, 28, 12, **(2008)**.

[9] G. Annapoorani, R. Krishnamoorthi and P. Gifty Jeya, "Accurate and fast iris segmentation", IEEE Computer Society Conference on Computer Vision and Pattern Recognition Workshops, 6, 2, **(2010)**.

[10] F. Scotti and V. Piuri, "Adaptive reflection detection and location in iris biometric images by using computational intelligence techniques", IEEE Transactions on Instrumentation and Measurement, 59, 7, **(2010)**.

[11] J. Daugman, "Iris recognition", American Scientist, 4, 89, **(2001)**.

[12] J. Daugman, "Complete discrete 2-D Gabor transforms by neural networks for image analysis and compression", IEEE Transactions on Acoustics, Speech, and Signal Processing, 36, 7, **(1988)**.

[13] http://www.cbsr.ia.ac.cn/IrisDatabase.htm [CASIA v3.0].

[14] http://www.bath.ac.uk/eleceng/research/sipg/irisweb/in dex.htm [Bath].

[15] http://pesona.mmu.edu.my/~ccteo/ [MMUv1.0].

[16] http://www.cbsr.ia.ac.cn/IrisDatabase.htm [CASIA v1.0].

[17] http://biometrics.idealtest.org/dbDetailForUser.do?id=1.

Authors

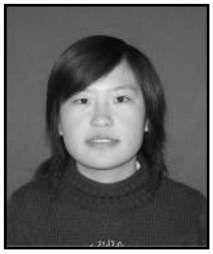

Chunxian Song

She received her bachelor degree in North China Institute of Aerospace Engineering, 2010. Currently she is a master candidate in China Three Gorges University and working for Institute of Intelligent vision and Image Information. Her areas of interest are Iris recognition, Pattern recognition and Computer vision. Email: songchunxian0419@163.com.

Guangzhu Xu

He is currently an associate Professor at University of China Three Gorges University, in the College of Computer and Information Technology & the Institute of Intelligent Vision and Image Information. He received his M.S. and Ph.D. degrees in Circuits & Systems and Radio Physics at Lanzhou University in 2004 and 2007. His main research interests are Biometrics, Computer vision and Pattern recognition. Email: xugzhu@gmail.com.

Chunlin Li

She received her bachelor degree in North China Institute of Aerospace Engineering, 2010. Currently she is a Master candidate in China Three Gorges University and working for Institute of Intelligent vision and Image Information. Her areas of interest are neural network and its application, Images processing, Pattern recognition and Machine vision. Email: lichunlin0921@126.com.

Jing Jing

She received her bachelor degree in China Three Gorges University, 2011. Currently she is a Master candidate in the university and working for Institute of Intelligent vision and Image Information. Her areas of interest are Images processing, Pattern recognition and Machine vision. Email: jingjinzhengxi@163.com.